

Effects of nanotube alignment and measurement direction on percolation resistivity in single-walled carbon nanotube films

Ashkan Behnam, Jing Guo, and Ant Ural^{a)}

Department of Electrical and Computer Engineering, University of Florida, Gainesville, Florida 32611

(Received 16 April 2007; accepted 3 July 2007; published online 28 August 2007)

We have used Monte Carlo simulations to study the effects of nanotube alignment and measurement direction on the resistivity in single-walled carbon nanotube films. These films consist of multiple layers of conductive nanotube networks with percolative transport as the dominant conduction mechanism. We find that minimum resistivity occurs for a partially aligned rather than a perfectly aligned nanotube film. When nanotubes are strongly aligned, the film resistivity becomes highly dependent on the measurement direction. We also find that aligning the nanotubes too strongly or measuring the resistivity in a direction which is very different from the alignment direction causes the film to approach the percolation threshold, as evidenced by the inverse power law increase in resistivity. Furthermore, the location of the resistivity minimum and the values of the inverse power law critical exponents are not universal, but depend strongly on other nanotube and device parameters. To illustrate this explicitly, we have studied the effect of three parameters, namely, nanotube length, nanotube density per layer, and device length on the scaling of nanotube film resistivity with nanotube alignment and measurement direction. We find that longer nanotubes, denser films, and shorter device lengths decrease the alignment critical exponent and the alignment angle at which minimum resistivity occurs, but increase the measurement direction critical exponent. However, the amount of increase or decrease in the critical exponents or the minima locations is different for each parameter. We explain these results by simple physical and geometrical arguments. Characterizing and understanding the effects of alignment and measurement direction on the percolation resistivity in films and composites made up of one-dimensional conductors, such as nanotubes, give valuable insights into the optimal way to arrange these nanomaterials for potential applications in optoelectronics, sensors, and flexible microelectronics.

© 2007 American Institute of Physics. [DOI: [10.1063/1.2769953](https://doi.org/10.1063/1.2769953)]

I. INTRODUCTION

Single-walled carbon nanotube (CNT) two-dimensional (2D) networks and three-dimensional (3D) films are promising materials for device applications due to the fact that they are simultaneously transparent, conductive, and flexible.^{1,2} They also exhibit uniform physical and electronic properties since individual variations in nanotube diameter and chirality^{3,4} are ensemble averaged.^{1,4-6} As a result, the reproducibility and reliability problems found in devices based on individual nanotubes are not observed in CNT film based devices, and they can be mass produced in a cost effective manner.^{5,7} Several promising applications of CNT films have recently been demonstrated, such as thin film transistors,^{8,9} flexible microelectronics,^{10,11} chemical sensors,¹²⁻¹⁵ and optoelectronic devices.¹⁶⁻²⁰

One of the significant characteristics of nanotube films, which needs to be considered in any device application, is that their resistivity depends strongly on nanotube and device parameters due to percolative conduction through the film.^{5,7,21,22} For example, by patterning CNT films down to submicron dimensions using e-beam lithography and inductively coupled plasma (ICP) etching,²³ we have recently

shown that the resistivity of CNT films exhibits an inverse power law dependence on device width and film thickness near the percolation threshold.²⁴

Another important parameter that significantly affects the percolation resistivity of CNT films is the nanotube alignment within the film. Typically, the nanotubes in CNT films are randomly oriented in the plane of the substrate on which they are deposited, as shown in the atomic force microscopy image of Fig. 1(a). There has been a great deal of recent research interest in aligning single-walled carbon nanotubes, either individually or in a thin film network or composite.²⁵⁻³⁰ For example, in a recent experimental work, it was found that the resistivity of nanotube/polymer composites depends strongly on nanotube alignment in the composite.²⁷ Also, very recently, well-aligned dense networks of nanotubes have been grown on quartz wafers and used as the channel material in thin film transistors.^{29,30} The performance of these transistors was studied using a numerical stick-percolation-based model.³⁰ There have been a few other theoretical studies on the conductivity of networks and composites made up of conducting “sticks,” but with an emphasis on investigating the effect of stick alignment on the percolation threshold.³¹⁻³³ In addition, we have recently studied the effect of various nanotube parameters on the resistivity scaling of CNT films with device width using Monte Carlo simulations.³⁴ However, a systematic and detailed

^{a)}Author to whom correspondence should be addressed. Electronic mail: antural@ufl.edu

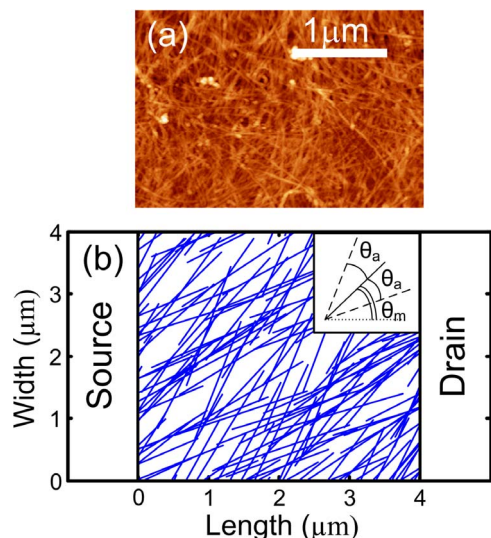


FIG. 1. (Color online) (a) Atomic force microscope (AFM) image of a nanotube film with an approximate thickness of $t=15$ nm where nanotubes are randomly distributed. (b) A 2D nanotube network generated using a Monte Carlo process for a device with device length $L=4$ μm, device width $W=4$ μm, $l_{\text{CNT}}=2$ μm, $n=2$ μm⁻², and $t=15$ nm. In this case, the nanotube alignment angle $\theta_a=27^\circ$ and the measurement direction angle $\theta_m=45^\circ$, where the definition of the two angles are illustrated in the inset.

study of the effects of nanotube alignment and measurement (channel) direction on the resistivity of CNT films and the effects of various nanotube and device parameters on the scaling of film resistivity with nanotube alignment and measurement direction has not been reported previously. This effect of alignment is especially unexplored for thicker 3D nanotube films with nanotube length shorter than the device (channel) length, where the conduction is dominated by percolation-type transport. Although such thick films are not usually used in “gate-modulated” transistor-type devices, they are very promising as transparent, conductive, and flexible electrodes in optoelectronic devices,^{1,16-20} and as chemical and biological sensors.¹²⁻¹⁵ As a result, a better understanding of alignment and measurement direction-dependent resistivity and its dependence on other nanotube and device parameters would give valuable insights into the optimal way to arrange the nanotubes in CNT films and would offer guidance to future applications in optoelectronics, sensors, and flexible microelectronics.

In this paper, we first study the effects of nanotube alignment and measurement direction on the resistivity of CNT films in detail by randomly generating the nanotubes using Monte Carlo simulations and calculating the resistivity. Our films consist of multiple layers of conductive nanotube networks with the device (channel) length always larger than the nanotube length, resulting in percolation transport. We find that, in agreement with previous observations,^{27,30} the resistivity minimum occurs for a partially aligned rather than a perfectly aligned nanotube film. In other words, contrary to what one might initially expect, more alignment does not always lead to a resistivity decrease. Furthermore, when nanotubes are strongly aligned, the film resistivity becomes highly dependent on the measurement direction. In addition, we find that aligning the tubes too strongly or measuring the

resistivity in a direction which is very different from the alignment direction causes the film to approach the percolation threshold, as evidenced by the inverse power law increase in resistivity. Furthermore, the location of the resistivity minimum and the values of the inverse power law critical exponents are not universal, but depend strongly on other device and nanotube parameters. As a result, we have also studied the effect of three parameters, namely, nanotube length, nanotube density per layer, and device length on the variation of CNT film resistivity with nanotube alignment and measurement direction. We find that longer nanotubes, denser films, and shorter device lengths decrease the alignment critical exponent and the alignment angle at which minimum resistivity occurs, but increase the measurement direction critical exponent. However, the amount of increase or decrease is different for each parameter. We explain these simulation results by simple physical and geometrical arguments. Our simulation results presented here are not limited to carbon nanotubes, but are, in general, applicable to a broader range of problems involving percolating transport in networks, nanocomposites, or films made up of one-dimensional conductors, such as nanotubes, nanowires, and nanorods.

II. COMPUTATIONAL APPROACH

Simulation of the electrical properties of the nanotube film was performed by randomly generating the nanotubes using a Monte Carlo process. The procedure for generating the film and calculating the resistivity has been explained in detail previously.³⁴ Briefly, each nanotube in the film is modeled as a stick with fixed length l_{CNT} and two degrees of freedom (position of one end of the nanotube and its direction). Nanotubes are generated at random angles θ with respect to the horizontal axis, where θ is limited to the range $\theta_m - \theta_a \leq \theta \leq \theta_m + \theta_a$ and $180 + \theta_m - \theta_a \leq \theta \leq 180 + \theta_m + \theta_a$. The first angle θ_a is defined as the “nanotube alignment angle,” which is a measure of the degree of nanotube alignment in the film. When $\theta_a=90^\circ$, the nanotubes are completely randomly distributed, whereas when $\theta_a=0^\circ$, they are completely aligned in a specific direction. The second angle θ_m , which we call the “measurement direction angle,” is the orientation of the nanotube alignment direction with respect to the resistivity measurement direction (i.e., the channel direction between the source and drain electrodes, which in our case is always chosen as the horizontal axis). When $\theta_m=0^\circ$, the resistivity is measured parallel to the alignment direction, while when $\theta_m=90^\circ$, it is measured perpendicular to the alignment direction. As an example, Fig. 1(b) shows a 2D nanotube film generated using our simulation code between the source and drain electrodes with $\theta_a=27^\circ$ and $\theta_m=45^\circ$, where the definition of the two angles is illustrated in the inset.

Random generation of the nanotubes on a 2D grid is repeated until the desired value for the nanotube density per layer n is achieved. Additional 2D layers are generated using the same approach and stacked on top of each other to form a 3D film. It is assumed that only nanotubes in nearest neighbor 2D layers form junctions, and the locations of these junc-

tions are determined by the simulation code. As a result, the effective integrated density of a 3D film consisting of l layers of density n per layer is always less than ln , since only nanotubes in nearest neighbor 2D layers are electrically connected. In general, the relationship between n and the effective integrated density depends on other device and nanotube parameters, and cannot be expressed in a simple analytic form.

After the film generation is completed, the locations of the junctions between nanotubes in the film (which we refer to as “nodes”) are determined. Based on recent studies on the electron transport through nanotube junctions,^{35–38} the contact resistance at tube-tube junctions depends on the type of the junction (i.e., metallic/semiconducting, semiconducting/semiconducting, or metallic/metallic),³⁵ and also on the atomic structure in the contact region.³⁶ In our simulations, each tube-tube junction is modeled by an “effective” contact resistance R_{JCT} regardless of the type of junction, following the simplified approach of Refs. 22 and 34. As the next step, the locations of the neighbors of each node (i.e., other nodes that are in direct electrical contact with that node) are located, and the resistance between two neighboring nodes is determined by a model that takes into account the ballistic transport in individual nanotube segments.^{34,39,40} Writing Kirchoff’s current law (KCL) at each node with the node voltage as the unknown and the voltages applied to the source/drain electrodes as the boundary conditions, the voltage at each node is determined. The total current in the film is calculated by a summation over the currents flowing into the drain, and the resistivity ρ of the nanotube film in the linear regime is calculated.

For each data point presented in this paper, 200 or more independent nanotube film configurations were randomly generated and their results were averaged in order to remove statistical variations due to different realizations of the nanotube film. The resistivity values presented throughout this paper have been normalized for easier comparison of the relative resistivity magnitudes.

For our simulations, we have used a device length of $L=7\ \mu\text{m}$, device width of $W=2\ \mu\text{m}$, nanotube density per layer of $n=2\ \mu\text{m}^{-2}$, nanotube length of $l_{\text{CNT}}=2\ \mu\text{m}$, and five stacked 2D nanotube layers, which is estimated to correspond to a film thickness of $t=15\ \text{nm}$.³⁴ Furthermore, the ratio of the tube-tube junction contact resistance R_{JCT} to the theoretical nanotube contact resistance at the ballistic limit ($\sim 6.5\ \text{k}\Omega$) was taken as 100, which is the value previously extracted from the simulation best fit of the experimental resistivity versus device width data.^{24,34} These parameters are used for all of the simulations in this paper, unless otherwise indicated.

Despite the relative simplicity of our model, our simulation results presented below provide valuable physical insights into the alignment and measurement direction-dependent percolation resistivity in CNT films and its dependence on other nanotube and device parameters, as well as capture the experimentally observed effects of nanotube alignment in nanotube/polymer composites.

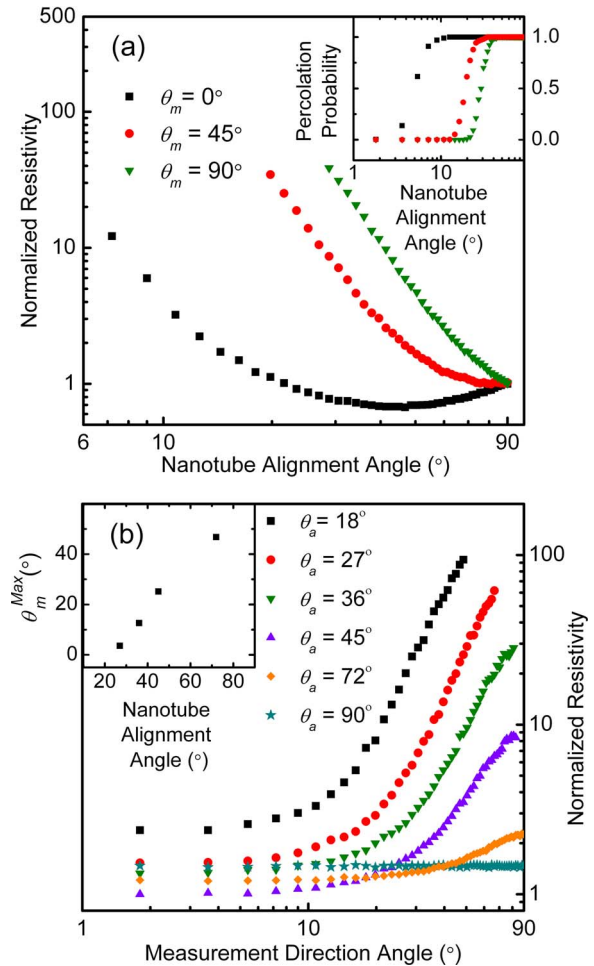


FIG. 2. (Color online) (a) Log-log plot of normalized resistivity vs nanotube alignment angle for three measurement direction angles ranging from 0° to 90° , labeled by different symbols. Device length $L=7\ \mu\text{m}$, device width $W=2\ \mu\text{m}$, $l_{\text{CNT}}=2\ \mu\text{m}$, $n=2\ \mu\text{m}^{-2}$, and $t=15\ \text{nm}$. The inset shows the percolation probability vs nanotube alignment angle θ_a for the same set of θ_m . (b) Log-log plot of normalized resistivity vs measurement direction angle for six nanotube alignment angles ranging from 18° to 90° . The values of the measurement direction critical exponents β extracted from the slope of the ρ vs θ_m curves near the percolation threshold (i.e., at large θ_m) are $\beta = 2.9, 2.9, 2.7, 1.85, 0.65, \text{ and } 0$ for $\theta_a = 18^\circ, 27^\circ, 36^\circ, 45^\circ, 72^\circ, \text{ and } 90^\circ$, respectively. Films with a high degree of alignment (i.e., $\theta_a = 18^\circ$ and 27°) are completely disconnected as we approach $\theta_m = 90^\circ$. The inset shows θ_m^{Max} vs θ_a .

III. RESULTS AND DISCUSSION

A. Resistivity versus nanotube alignment angle

Figure 2(a) shows the plot of normalized resistivity versus nanotube alignment angle for three different measurement direction angles ($\theta_m = 0^\circ, 45^\circ, \text{ and } 90^\circ$). It is evident that for $\theta_m = 0^\circ$, the resistivity slowly decreases as θ_a is reduced, and reaches a minimum value at $\theta_a \sim 45^\circ$, which we define as θ_a^{Min} , the nanotube alignment angle at which minimum resistivity occurs. This can be explained by the fact that, as the nanotubes become more aligned, they form conduction paths with fewer junctions and shorter lengths between the source and drain. However, as θ_a is further reduced, resistivity starts to increase significantly. This is due to the fact that, as the nanotubes become even further aligned, the number of conduction paths begins to decrease significantly. For example, in the case of almost perfect

alignment, each nanotube forms only very few junctions with its neighbors, since it lies almost parallel to them. As a result of this competition between the decrease in the number of junctions and *lengths* of the conduction paths (which decreases the resistivity) and the decrease in the *number* of conduction paths (which increases the resistivity), the resistivity minimum occurs for a partially aligned rather than a perfectly aligned nanotube film.

In our simulations, the device length L is always larger than nanotube length l_{CNT} . As a result, a single nanotube can never connect source to drain. In this case, as we have seen above, strong alignment increases the resistivity. However, if the nanotube length was longer than the device length (i.e., $l_{\text{CNT}} > L$),²⁹ the source and drain could be connected by single nanotubes, and strong alignment of nanotubes would reduce the resistivity. Furthermore, in contrast to well-defined values of θ_a in our simulations, a few completely misaligned nanotubes that bridge perfectly aligned tubes can exist in experimentally aligned nanotube films and networks, reducing the resistivity significantly by introducing additional conduction paths.³⁰

The effect of the measurement direction angle θ_m on the resistivity scaling with nanotube alignment is also depicted in Fig. 2(a). When $\theta_a = 90^\circ$, nanotubes have completely random orientation, and the value of resistivity is independent of the measurement direction angle θ_m . As a result, the curves for $\theta_m = 0^\circ, 45^\circ$, and 90° intersect, as shown in Fig. 2(a). In contrast to the case when $\theta_m = 0^\circ$, for $\theta_m = 45^\circ$ and 90° , as θ_a decreases, the resistivity increases continuously without exhibiting any minimum. In these latter two cases, since the measurement direction is not parallel to the alignment direction, the number of junctions and lengths of the conduction paths between the source and drain do not decrease significantly with more alignment. As a result, the reduction in the number of conduction paths dominates the resistivity change, and the resistivity continuously increases.

Figure 2(a) also shows that the resistivity exhibits an inverse power law dependence on θ_a as the film approaches the percolation threshold at small alignment angles, given by

$$\rho \propto \theta_a^{-\alpha}, \quad (1)$$

where $\alpha = 2.9, 3.6$, and 3.9 are the alignment critical exponents extracted from the slope of the log-log plots for $\theta_m = 0^\circ, 45^\circ$, and 90° , respectively. The alignment critical exponent α increases for large θ_m since the reduction in the number of conduction paths begins to dominate the resistivity change as θ_m increases. These results are in agreement with recent experimental work on the effect of nanotube alignment on percolation conductivity in carbon nanotube/polymer composites.²⁷

To complement the resistivity data, the inset of Fig. 2(a) shows the percolation probability P , defined as the probability that the nanotube film is conducting (i.e., the probability of finding at least one conducting path between the source and drain electrodes), versus nanotube alignment angle for the same set of θ_m . For measurement directions that are not parallel to the nanotube alignment direction, the percolation threshold (i.e., the transition point where the percolation probability drops from one to zero) occurs at higher values

of θ_a . This is due to the fact that it becomes more difficult to form a conduction path for strongly aligned films if the measurement direction is very different from the alignment direction. For example, for $\theta_m = 0^\circ$, the transition from $P = 1$ to 0 starts when θ_a becomes smaller than 10° , whereas for $\theta_m = 90^\circ$, it starts when θ_a gets lower than 40° .

B. Resistivity versus measurement direction angle

To illustrate the effect of the measurement direction angle from a different perspective, Fig. 2(b) shows the plot of normalized resistivity versus θ_m for six different values of θ_a ranging from 18° to 90° . It is evident from Fig. 2(b) that when the nanotubes are randomly distributed (i.e., $\theta_a = 90^\circ$), the resistivity is almost independent of θ_m . In contrast, even for slightly aligned tubes (such as $\theta_a = 72^\circ$), the resistivity starts to increase with increasing θ_m , and for well-aligned nanotubes (such as $\theta_a = 18^\circ$), this increase becomes very strong. Furthermore, the resistivity exhibits an inverse power law dependence on θ_m as the film approaches the percolation threshold at large measurement direction angles, given by

$$\rho \propto (90 - \theta_m)^{-\beta}, \quad (2)$$

where β is the measurement direction critical exponent. The value of β extracted from the slope of the log-log plots in Fig. 2(b) increases from 0.65 to 2.9 when θ_a goes from 72° to 18° , which is a manifestation of the stronger dependence of resistivity on θ_m as the nanotubes in the film become more aligned.

As a measure of the sensitivity of film resistivity to the measurement direction angle, we define θ_m^{Max} as the maximum θ_m above which the resistivity of an aligned film becomes larger than that of a completely random film (within $\pm 5\%$ error). In other words, θ_m^{Max} is a measure of the degree of misalignment in the measurement direction that can be tolerated before the aligned film becomes more resistive than a random film. By this definition, θ_m^{Max} is only meaningful for alignment angles at which the resistivity when $\theta_m = 0^\circ$ is lower than that of a completely random film, which is around $\theta_a = 22^\circ$ in our case, as seen from Fig. 2(a). The plot of θ_m^{Max} vs θ_a is shown in the inset of Fig. 2(b). We can see that θ_m^{Max} increases as the film becomes less aligned. This demonstrates once again that for well-aligned nanotubes, the film resistivity becomes very sensitive to the measurement direction.

C. Effects of device and nanotube parameters

The location of the resistivity minimum and the values of α and β are not universal, but depend strongly on other device and nanotube parameters. As a result, we now study the effect of three parameters, namely, nanotube length, nanotube density per layer, and device length on the scaling of resistivity as a function of θ_a and θ_m . The effects of these three parameters on the *absolute value* of resistivity, which is also visible in the figures of this section, have been explained in detail in our previous work.³⁴

1. Nanotube length

Figure 3(a) shows the plot of normalized resistivity versus nanotube alignment angle for three values of l_{CNT} when

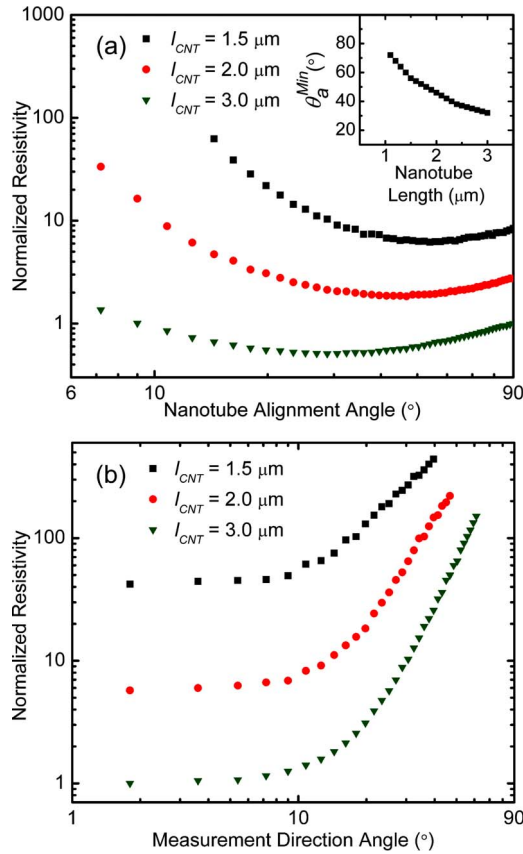


FIG. 3. (Color online) (a) Log-log plot of normalized resistivity vs nanotube alignment angle for three nanotube lengths ranging from 1.5 to 3 μm when $\theta_m=0^\circ$. Resistivity minima are located at $\theta_a^{\text{Min}} \sim 55^\circ$, 45° , and 30° and alignment critical exponent values are $\alpha=2.9$, 2.9, and 1.6 for $l_{CNT}=1.5$, 2, and 3 μm , respectively. The inset depicts θ_a^{Min} vs nanotube length. (b) Log-log plot of normalized resistivity vs measurement direction angle for three nanotube lengths ranging from 1.5 to 3 μm when $\theta_a=18^\circ$.

$\theta_m=0^\circ$. As the nanotube length is increased from $l_{CNT}=1.5$ to 3.0 μm , θ_a^{Min} decreases from 55° to 30° , and the critical exponent α decreases from 2.9 to 1.6. Longer nanotubes form more junctions with each other, and therefore, even when they are strongly aligned, the number of conducting paths is not reduced as strongly as in the case of shorter nanotubes. In other words, increasing the alignment does not eliminate as many conduction paths for longer tubes as it does for shorter ones. This shifts both θ_a^{Min} and α to lower values as l_{CNT} increases.

The inset of Fig. 3(a) shows θ_a^{Min} versus nanotube length. It is evident that as the nanotubes get shorter, the rate of change of θ_a^{Min} increases. A film consisting of shorter nanotubes is closer to the percolation threshold, and therefore, even a slight increase in alignment can remove a significant number of additional conduction paths from the film. As a result, for very short nanotubes, θ_a^{Min} approaches 90° .

Figure 3(b) shows the plot of normalized resistivity versus measurement direction angle for three values of l_{CNT} when $\theta_a=18^\circ$. We have used $\theta_a=18^\circ$ for the resistivity versus measurement direction angle plots in Figs. 3–5, since the effect of θ_m on resistivity is most pronounced for well-aligned nanotubes, as seen in Fig. 2(b). A lower θ_a value was not chosen since for lower nanotube alignment angles, the nanotube film falls below the percolation threshold even at

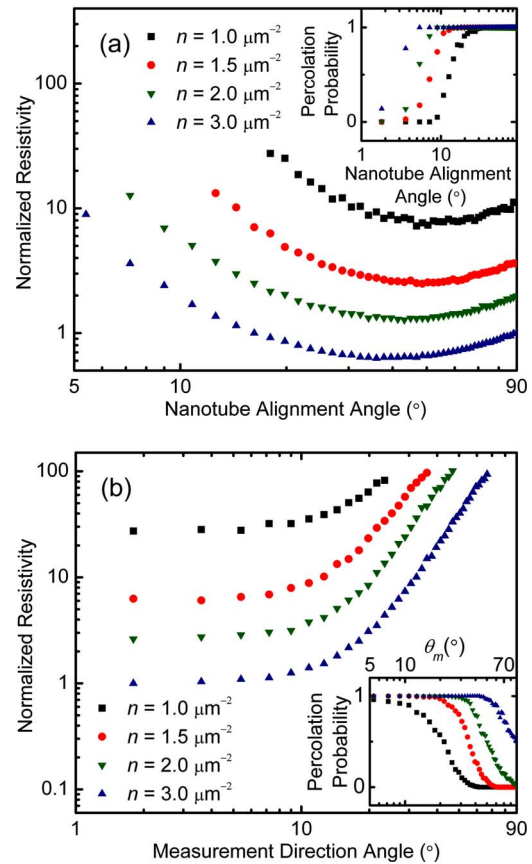


FIG. 4. (Color online) (a) Log-log plot of normalized resistivity vs nanotube alignment angle for four nanotube densities per layer ranging from 1 to 3 μm^{-2} when $\theta_m=0^\circ$. θ_a^{Min} values are located at $\sim 50^\circ$, 45° , 45° , and 40° and $\alpha=2.8$, 3.0, 2.9, and 2.9 for $n=1$, 1.5, 2, and 3 μm^{-2} , respectively. The inset shows the percolation probability vs nanotube alignment angle θ_a for the same set of n . (b) Log-log plot of normalized resistivity vs measurement direction angle for four nanotube densities per layer ranging from 1 to 3 μm^{-2} when $\theta_a=18^\circ$. The inset shows the percolation probability vs θ_m for the same set of n .

small values of θ_m . A higher θ_a value was not chosen, because at higher θ_a , the effect of the measurement direction on resistivity is not as pronounced as at $\theta_a=18^\circ$, and therefore the effects of device and nanotube parameters illustrated in Figs. 3–5 would not be as evident.

The measurement direction critical exponent β extracted from Fig. 3(b) shows an increase with increasing nanotube length ($\beta=1.7$, 2.9, and 3.75 for $l_{CNT}=1.5$, 2, and 3 μm , respectively). This is the opposite of the trend observed for α in Fig. 3(a). Since initially, the number of conduction paths is more for films with longer nanotubes, misaligning the measurement direction reduces the number of paths (and hence increases the resistivity) more rapidly than that for films with shorter nanotubes. This results in a larger β .

2. Nanotube density per layer

Figure 4(a) shows the plot of normalized resistivity versus nanotube alignment angle for four nanotube densities n ranging from 1 to 3 μm^{-2} when $\theta_m=0^\circ$. Compared to the case of nanotube length, θ_a^{Min} and α do not change as significantly when the nanotube density changes. This can be explained by the fact that increasing the nanotube length in-

increases the number of nanotubes in a 2D area element proportional to the square of the length, whereas increasing the density increases this number only linearly, as demonstrated previously.³⁴ This results in a larger change in both θ_a^{Min} and α as a function of the length of the nanotubes compared to that of their density. To compliment the resistivity data, the inset of Fig. 4(a) shows the percolation probability P versus nanotube alignment angle for the same set of densities, illustrating that the percolation threshold for alignment angle is also a function of density. For example, for $n = 1 \mu\text{m}^{-2}$, the transition from $P=1$ to 0 starts when θ_a becomes smaller than $\sim 30^\circ$, whereas for $n = 3 \mu\text{m}^{-2}$, it starts when θ_a gets lower than $\sim 5^\circ$.

Figure 4(b) shows the plot of normalized resistivity versus measurement direction angle for four nanotube densities at $\theta_a = 18^\circ$. The extracted measurement direction critical exponent values are $\beta = 1.4, 2.45, 2.9,$ and 3.0 for $n = 1, 1.5, 2,$ and $3 \mu\text{m}^{-2}$, respectively. This change of β with density is also less pronounced than that with nanotube length. The inset of Fig. 4(b) shows the percolation probability P versus measurement direction angle for the same set of densities, illustrating that the percolation threshold for measurement direction angle is also a strong function of density. For example, for $n = 1 \mu\text{m}^{-2}$, the transition from $P=1$ to 0 starts when θ_m becomes larger than $\sim 7^\circ$, whereas for $n = 3 \mu\text{m}^{-2}$, it starts when θ_m gets higher than $\sim 50^\circ$.

3. Device length

Finally, Fig. 5 shows the plot of normalized resistivity versus nanotube alignment angle for three device lengths L ranging from 2 to 7 μm when $\theta_m = 0^\circ$. From this figure, we extract $\theta_a^{\text{Min}} \sim 35^\circ, 45^\circ,$ and 45° and $\alpha = 0.9, 2.2,$ and 2.9 for $L = 2, 4,$ and $7 \mu\text{m}$, respectively. When the device length is shorter, the source and drain are connected by conduction paths consisting of only a few nanotubes in series. However, as the device length is increased, more nanotubes are necessary to form a conduction path, which is less likely to happen when the nanotubes become strongly aligned. Therefore, α is higher for longer device lengths compared to shorter ones. Similarly, θ_a^{Min} shifts to higher values for longer devices. The inset also depicts normalized resistivity versus measurement direction angle for two device lengths when $\theta_a = 18^\circ$. The critical exponents are $\beta = 4.9$ and 2.9 for $L = 2$ and $7 \mu\text{m}$, respectively. Similar to the previous case, for shorter devices, many conduction paths that have been formed between source and drain are removed as the measurement angle increases. Therefore, resistivity increases faster for shorter device lengths, and the critical exponent increases.

IV. CONCLUSIONS

In summary, we have used Monte Carlo simulations to study the effects of nanotube alignment and measurement direction on the percolation resistivity in CNT films. Our study has focused on thick nanotube films with the device length larger than the nanotube length, in which percolative transport is the dominant conduction mechanism. We find that the resistivity minimum occurs for a partially aligned rather than perfectly aligned nanotube film. In other words,

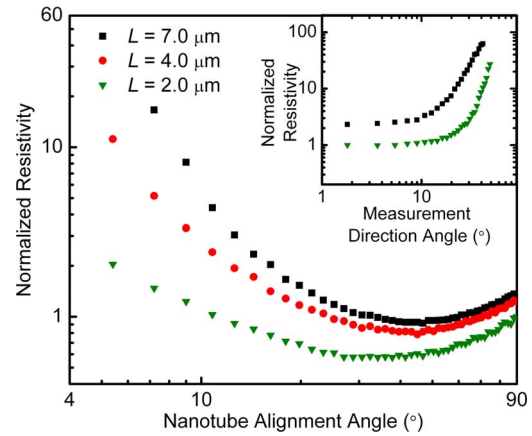


FIG. 5. (Color online) Log-log plot of normalized resistivity vs nanotube alignment angle for three device lengths ranging from $L = 2$ to $7 \mu\text{m}$, when $\theta_m = 0^\circ$. The inset depicts log-log plot of normalized resistivity vs measurement direction angle for two device lengths ($L = 2$ and $7 \mu\text{m}$) when $\theta_a = 18^\circ$.

more alignment does not always lead to a resistivity decrease. Furthermore, when the nanotubes are strongly aligned, the film resistivity becomes highly dependent on the measurement direction. In addition, aligning the nanotubes too strongly or measuring the resistivity in a direction which is very different from the alignment direction causes the film to approach the percolation threshold, as evidenced by the inverse power law increase in resistivity. These results are in agreement with recent experimental work on the effect of nanotube alignment on percolation conductivity in carbon nanotube/polymer composites and on the transport in thin nanotube network transistors. Furthermore, the location of the resistivity minimum and the values of the inverse power law exponents are not universal, but depend strongly on other device and nanotube parameters. Consequently, we have also studied the effects of three parameters, namely, nanotube length, nanotube density per layer, and device length on the scaling of CNT film resistivity with nanotube alignment and measurement direction. We find that longer nanotubes, denser films, and shorter device lengths all decrease the alignment critical exponent and the alignment angle at which minimum resistivity occurs, and increase the measurement direction critical exponent. However, the amount of increase or decrease is different for each parameter. We explain these simulation results by simple physical and geometrical arguments.

Our simulation results presented here are not limited to carbon nanotubes, but are, in general, applicable to a broader range of problems involving percolating transport in networks, nanocomposites, or films made up of one-dimensional conductors, such as nanotubes, nanowires, and nanorods. Characterizing and understanding the effects of alignment and measurement direction on the percolation resistivity in nanotube films are essential steps towards improving the properties of these materials for their potential use in a wide range of device applications.

ACKNOWLEDGMENTS

This work was funded in part by the Woodrow W. Everett, Jr. SCEE Development Fund in cooperation with the

Southeastern Association of Electrical Engineering Department Heads, and in part by a University of Florida Research Opportunity Incentive Seed Fund.

- ¹Z. Wu *et al.*, *Science* **305**, 1273 (2004).
- ²K. Bradley, J. C. P. Gabriel, and G. Grüner, *Nano Lett.* **3**, 1353 (2003).
- ³M. Dresselhaus, G. Dresselhaus, and Ph. Avouris, *Carbon Nanotubes: Synthesis, Structure, Properties and Applications* (Springer, Berlin, 2001).
- ⁴J. Liu, S. Fan, and H. Dai, *MRS Bull.* **29**, 244 (2004).
- ⁵E. S. Snow, J. P. Novak, P. M. Campbell, and D. Park, *Appl. Phys. Lett.* **82**, 2145 (2003).
- ⁶Y. Zhou, L. Hu, and G. Grüner, *Appl. Phys. Lett.* **88**, 123109 (2006).
- ⁷E. Bekyarova, M. E. Itkis, N. Cabrera, B. Zhao, A. P. Yu, J. B. Gao, and R. C. Haddon, *J. Am. Chem. Soc.* **127**, 5990 (2005).
- ⁸T. Ozel, A. Gaur, J. A. Rogers, and M. Shim, *Nano Lett.* **5**, 905 (2005).
- ⁹R. Siedel, A. P. Graham, E. Unger, G. S. Duesberg, M. Liebau, W. Steinhögl, F. Kreupl, and W. Hoenlein, *Nano Lett.* **4**, 831 (2004).
- ¹⁰E. S. Snow, P. M. Campbell, and M. G. Ancona, *Appl. Phys. Lett.* **86**, 033105 (2005).
- ¹¹G. B. Blanchet, S. Subramony, R. K. Bailey, G. D. Jaycox, and C. Nuckolls, *Appl. Phys. Lett.* **85**, 828 (2004).
- ¹²L. Valentini, I. Armentano, J. M. Kenny, C. Cantalini, L. Lozzi, and S. Santucci, *Appl. Phys. Lett.* **82**, 961 (2003).
- ¹³J. S. Oakley, H. T. Wang, B. S. Kang, Z. Wu, F. Ren, A. G. Rinzler, and S. J. Pearton, *Nanotechnology* **16**, 2218 (2005).
- ¹⁴J. P. Novak, E. S. Snow, E. J. Houser, D. Park, J. L. Stepnowski, and R. A. McGill, *Appl. Phys. Lett.* **83**, 4026 (2003).
- ¹⁵E. S. Snow, F. K. Perkins, E. J. Houser, S. C. Badescu, and T. L. Reinecke, *Science* **307**, 1942 (2005).
- ¹⁶K. Lee, Z. Wu, Z. Chen, F. Ren, S. J. Pearton, and A. G. Rinzler, *Nano Lett.* **4**, 911 (2004).
- ¹⁷A. D. Pasquier, H. E. Unalan, A. Kanwal, S. Miller, and M. Chhowalla, *Appl. Phys. Lett.* **87**, 203511 (2005).
- ¹⁸C. M. Aguirre, S. Auvray, S. Pigeon, R. Izquierdo, R. Desjardins, and R. Martel, *Appl. Phys. Lett.* **88**, 183104 (2006).
- ¹⁹M. W. Rowell, M. A. Topinka, M. D. McGehee, H. J. Prall, G. Dennler, N. S. Sariciftci, L. Hu, and G. Grüner, *Appl. Phys. Lett.* **88**, 233506 (2006).
- ²⁰D. Zhang, K. Ryu, X. Liu, E. Polikarpov, J. Ly, M. E. Tompson, and C. Zhou, *Nano Lett.* **6**, 1880 (2006).
- ²¹D. Hecht, L. Hu, and G. Grüner, *Appl. Phys. Lett.* **89**, 133112 (2006).
- ²²S. Kumar, J. Y. Murthy, and M. A. Alam, *Phys. Rev. Lett.* **95**, 066802 (2005).
- ²³A. Behnam, Y. Choi, L. Noriega, Z. Wu, I. Kravchenko, A. G. Rinzler, and A. Ural, *J. Vac. Sci. Technol. B* **25**, 348 (2007).
- ²⁴A. Behnam, L. Noriega, Y. Choi, Z. Wu, A. G. Rinzler, and A. Ural, *Appl. Phys. Lett.* **89**, 093107 (2006).
- ²⁵A. Ural, Y. Li, and H. Dai, *Appl. Phys. Lett.* **81**, 3464 (2002).
- ²⁶E. Joselevich and C. M. Lieber, *Nano Lett.* **2**, 1137 (2002).
- ²⁷F. Du, J. E. Fisher, and K. I. Winey, *Phys. Rev. B* **72**, 121404(R) (2005).
- ²⁸M. D. Lynch and D. L. Patrick, *Nano Lett.* **2**, 1197 (2002).
- ²⁹S. J. Kang *et al.*, *Nat. Nanotechnol.* **2**, 230 (2007).
- ³⁰C. Kocabas, N. Pimparkar, O. Yesilyurt, S. J. Kang, M. A. Alam, and J. A. Rogers, *Nano Lett.* **7**, 1195 (2007).
- ³¹M. Foygel, R. D. Morris, D. Anez, S. French, and V. L. Sobolev, *Phys. Rev. B* **71**, 104201 (2005).
- ³²I. Balberg and N. Binenbaum, *Phys. Rev. B* **28**, 3799 (1983).
- ³³T. Natsuki, M. Endo, and T. Takahashi, *Physica A* **352**, 498 (2005).
- ³⁴A. Behnam and A. Ural, *Phys. Rev. B* **75**, 125432 (2007).
- ³⁵M. S. Fuhrer *et al.*, *Science* **288**, 494 (2000).
- ³⁶A. Buldum and J. P. Lu, *Phys. Rev. B* **63**, 161403(R) (2001).
- ³⁷J. W. Park, J. Kim, and K. H. Yoo, *J. Appl. Phys.* **93**, 4191 (2003).
- ³⁸H. W. Postma, M. Jonge, Z. Yao, and C. Dekker, *Phys. Rev. B* **62**, 10653(R) (2001).
- ³⁹S. Li, Z. Yu, C. Rutherglen, and P. J. Burke, *Nano Lett.* **4**, 2003 (2004).
- ⁴⁰J.-Y. Park *et al.*, *Nano Lett.* **4**, 517 (2004).